Optical Signatures of the Outer Radiation Belt Boundary

Nithin Sivadas, Joshua L. Semeter, Toshi Nishimura, Sebastijan Mrak

Centre for Space Physics and Department of Electrical and Computer Engineering, Boston University

Contact: nithin@bu.edu

Boston University Center for Space physics

1. Abstract

We present observations that show structured diffuse aurora (SDA) correlated with precipitation from the outer boundary of the outer radiation belt. Electrons of 100-300 keV lost from the boundary can cause ionization down to 70 km (ionospheric D-region) and can result in enhanced ionospheric conductance. Previous studies have not revealed clear optical signatures associated with the radiation belt boundary during substorm growth-phases. The Global airglOW (GLOW) model shows significant optical contributions (up to ~46%) from electrons > 30 keV within the SDA. Ground– and space-based measurements are consistent with the conclusion that the SDA marks the outer radiation belt boundary during substorm growth-phase. This result opens up a promising avenue for remote-sensing the radiation belt boundary and studying its effect on the ionosphere.

2. Motivation

Ionospheric signatures of plasma boundaries in the magnetosphere are useful indicators of the magnetospheric configuration. The plasma and energy flowing through them are of interest from an M-I coupling perspective. Enhanced ionization due to precipitation, can be measured using riometers and incoherent scatter radars (ISR), however, they have a narrow field of view (FOV). All-sky cameras on the other hand can observe optical signatures of precipitation over a large FOV. Hence we set out to **1) identify optical signatures associated with the radiation belt boundary** in all-sky cameras and **2) investigate the source mechanism leading to the precipitation**.

Significance

Quantifying the contribution of radiation belt precipitation towards detectable optical emissions is important in understanding sources of aurora. The ionospheric effects of the precipitation, e.g. enhanced D-region ionization and increased ionospheric conductance, can add substantial corrections to global precipitation and conductance models [1]. The spatial structure, and energy spectra of the precipitation, can be used as a remote-sensing tool for the outer radiation belt boundary location as well as the plasma processes within it.

3. Previous Work

Energetic precipitation during substorm growth-phases from the outer radiation belt boundary has been previously identified using LEO spacecraft. Termed Energetic Electron Arc (EEA), they are understood to be caused by current-sheet scattering—identified by their characteristic latitudinal energy dispersion signature [2]. Ionospheric signatures of this precipitation were observed through riometers as 'absorption arcs' with enhanced D-region conductivity. They were discussed as a signature of the 'stable trapping boundary' by *Kirkwood & Eliasson* [3]. However, optical signatures associated with the EEA have not been identified in previous literature except for one mention of a faint optical arc in overexposed images coincident with an absorption arc by Opgenoorth et al. [4]. No direct connection or correlation between optical signatures in the ionosphere and the radiation belt precipitation have been established yet.

4. Methodology

- The energetic precipitation was identified from low-altitude ionization reaching ~ 70 km with Poker Flat Incoherent Scatter Radar (**PFISR**) during a substorm growth-phase on 26 March 2008.
- The precipitation was identified also within the magnetosphere using electron flux measurements from **NOAA-17** in LEO.
- **T96** magnetic field model was used to map its source to be within the night-side transition region.
- **THEMIS-D** and –E spacecraft near the equatorial plane were used to evaluate the magnetic field model accuracy.
- 2-D **energy flux maps** of precipitation were estimated using PFISR ionization profiles [5] and were used to identify the source of the precipitation.
- **Optical cameras** observed the optical emissions of the SDA. Its correlation with energetic electron flux was established using a spatial correlation analysis.
- The **GLOW** model was used to estimate the contribution of energetic electrons to the optical emissions measured by the cameras.

5. Overview

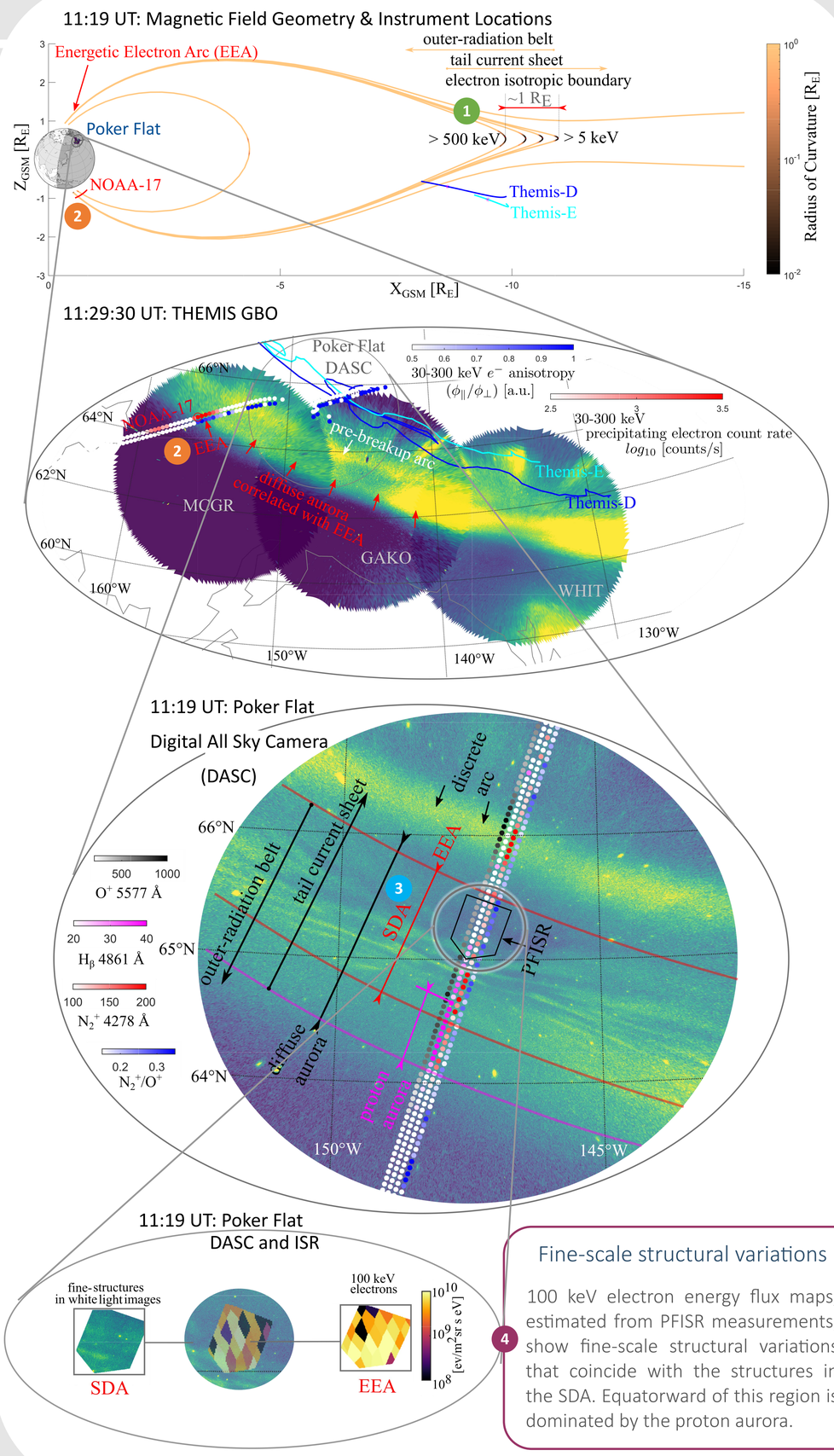

Current sheet scattering in a thinning plasmasheet

1 During the growth phase, the magnetic field lines stretch such that the radius of curvature near the equatorial plane is comparable to gyro-radius of energetic electrons > 5—500 keV in the night-side transition region. This results in current sheet scattering, that scatters electrons into the loss-cone.

Energetic precipitation from the transition region

2 NOAA-17 spacecraft observed energetic electrons precipitating in LEO from the outer radiation belt boundary. The spacecraft was in the southern hemisphere, with its northern magnetic foot point coinciding with diffuse aurora equatorward of the pre-breakup arc at 11:29:30 UT.

Energetic precipitation coincident with SDA

3 A closer look through Poker Flat Digital All-sky Camera (DASC) 10 minutes earlier shows structure in the poleward shoulder of the diffuse aurora, correlated with O^+/N_2^+ emission ratios. The structured diffuse aurora (SDA) maps to the night-side transition region where plasma from both the radiation belt and the plasmasheet co-exist.

Fine-scale structural variations

4 100 keV electron energy flux maps, estimated from PFISR measurements, show fine-scale structural variations that coincide with the structures in the SDA. Equatorward of this region is dominated by the proton aurora.

6. Results

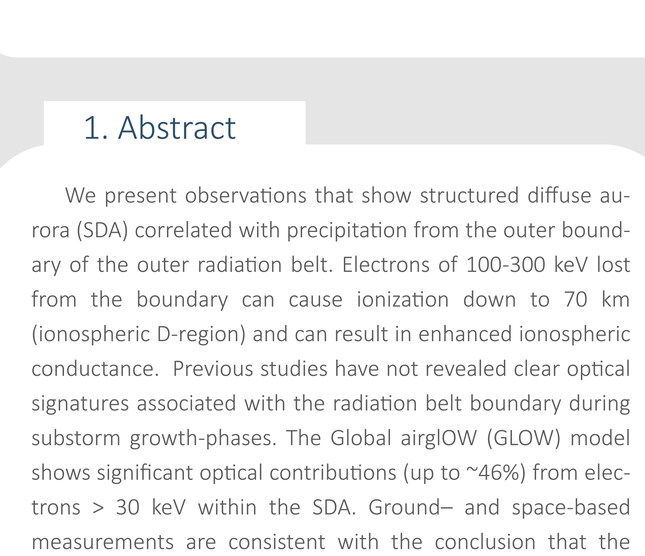

Energetic Electron Precipitation during Growth-phase caused by Current Sheet Scattering

Panel a) of the above figure shows a keogram within PFISR field of view (FOV). The three lines are latitudes of the peak energy flux of precipitating electrons of 30, 70 and 100 keV. There is a latitudinal dispersion of energy with higher energies more equatorward. This is consistent with the criteria for non-adiabatic current sheet scattering ($K_c = R_{cmin}/\rho < 8$) along the conjugate magnetic field line where K_c is the ratio of minimum radius of curvature (R_{cmin}) and gyro-radius of the charged particle (ρ) [2].

Precipitating Energetic Electrons contribute substantially to Optical Emissions

Panel b) shows the emission intensities of 4278 Å produced by electrons >30 keV and >100 keV estimated using energy fluxes from PFISR as input to the GLOW model. Electrons >30 keV generate a maximum of about 400 Rayleigh (46% of total emissions), which is detectable by scientific cameras.

Panel c) shows quantitative estimates of the energy flux, with >30 keV electrons reaching ~1 mWm^{-2}—which is considered high enough to be detectable by standard white light cameras. Electrons <30 keV have higher energy fluxes ~3 mWm^{-2}, which implies that they dominate the optical emissions. The electrons >30 keV are likely part of the radiation belt population, while electrons <30 keV are part of the plasmasheet.

Optical Signatures correlated with the Outer Radiation Belt Boundary

Panel d) shows the spatial correlation coefficient of energy flux of different energies with optical emissions. In the early growth-phase, higher energy precipitation (>100 keV) is correlated with the optical emissions. From 11:12 UT the fine structures of the structured diffuse aurora is correlated with ~100 keV electrons with the correlated energy decreasing with time. This is consistent with the latitudinal energy dispersion within the SDA, manifesting in time (11:12-11:24 UT) as the aurora moves equatorward at a rate of ~5 km/min over the PFISR FOV. Note that the optical emissions are also correlated with ~10 keV electrons during the same time. These are likely scattered from the inner plasma sheet that overlaps with the outer boundary of the radiation belt, and continues poleward.

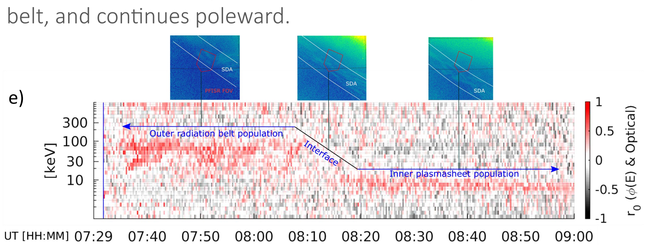

Panel e) shows a different growth phase event on 18th Oct 2010, during which one can see the different electron populations and their relative positions with respect to the SDA. The outer radiation belt boundary and the interface region coincides with the SDA, while most of the inner plasma sheet is poleward of it.

7. Conclusion

- SDA during a strong substorm growth-phase marks the outer boundary of the radiation belt. This may be used as a remote-sensing diagnostic of the radiation belt boundary.
- 30-300 keV electrons precipitating from the region of the outer radiation belt boundary overlapping with the inner plasmasheet contributes up to 46% of the 4278 Å emissions.
- Current sheet scattering is one of the mechanisms that cause the precipitation. However, other acceleration mechanisms such as wave-particle interactions cannot be ruled out.
- The structure precipitation from the interface region between the outer radiation belt and inner plasmasheet may be a result of plasma wave instabilities in the thin current sheet.

References:

[1] Yu, Y., Jordanova, V. K., McGranghan, R. M., Solomon S. C. (2018). Self-Consistent Modeling of Electron Precipitation and Responses in the Ionosphere: Application to Low-Altitude Energization During Substorms, *Geophysical Research Letters*, 45 (13), 6371-6381.

[2] Sergeev, V. A., Sazhina, E., Tsyganenko, N., Lundblad, J., & Sraas, F. (1983). Pitch-angle scattering of energetic protons in the magnetotail current sheet as the dominant source of their isotropic precipitation into the nightside ionosphere. *Planetary and Space Science*, 31 (10), 1147-1155.

[3] Kirkwood, S., & Eliasson, L. (1990). Energetic Particle Precipitation in the Substorm Growth Phase Measured by EISCAT and Viking. *Journal of Geophysical Research*, 95 (A5), 6025-6037.

[4] Opgenoorth, H. J., Pellinen, R. J., Baumjohann, W., Nielsen, E., Marklund, G., & Eliasson, L. (1983). Three-dimensional current flow and particle precipitation in a westward travelling surge (observed during the Barium-Geos Rocket Experiment). Journal of Geophysical Research, 88 (A

[5] Sivadas, N., Semeter, J., Nishimura, Y., & Kero, A. (2017). Simultaneous Measurements of Substorm-Related Electron Energization in the Ionosphere and the Plasma Sheet. Journal of Geophysical Research: Space Physics, 448 122 (10), 10,528-10,547.

[6] Gustavsson, B., U. Brändström, and M. Hirsch (2016), AIDA-tools: ALIS auroral tomography Matlab software suite [Data Set], , doi:10.5281/zenodo.213308

[7] Sergienko, T. I., Ivanov, V. E.: A new approach to calculate the excitation of atmospheric gases by auroral electron impact, Ann. Geophysica, 11, 717-727, 1993.

Acknowledgements: This work was supported by NASA Headquarters under the NASA Earth and Space Science Fellowship Program Grant—80NSSC17K0433. PPFISR operations are supported by National Science Foundation Cooperative Agreement AGS-1133009 to SRI international. Additionally, we recognize the use of AIDA-tools [6] to run the Monte Carlo simulations by *Sergienko and Ivanov* [7]. N. Sivadas wishes to thank V. Sergeev, L. Lyons, R. Varney, A. Reimer, P. Reyes, M. Samara, W. Li, E. A. McDonald, D. G. Sibeck and M. Oppenheim for helpful discussions. We acknowledge the use of IRBEM Library V4.3, 2004-2008 for magnetic field models. We acknowledge NASA contract NAS5-2099 and V. Angelopoulos for use of data from the THEMIS mission, and specifically S. Mende and E. Donovan for use of the ASI data.